Trends in Cardiovascular Medicine 35 (2025) 47–59

Contents lists available at ScienceDirect

Trends in Cardiovascular Medicine

journal homepage: www.elsevier.com/locate/tcm

# Enhancing cardiovascular risk stratification: Radiomics of coronary plaque and perivascular adipose tissue – Current insights and future perspectives

Anna Corti[a,1,*], Francesca Lo Iacono[a,1], Francesca Ronchetti[b], Saima Mushtaq[b], Gianluca Pontone[b,d], Gualtiero I. Colombo[c], Valentina D.A. Corino[a,b]

[a] Department of Electronics, Information and Bioengineering, Politecnico di Milano, Via Ponzio 34/5, Milan 20133, Italy
[b] Department of Perioperative Cardiology and Cardiovascular Imaging, Centro Cardiologico Monzino IRCCS, Milan, Italy
[c] Unit of Immunology and Functional Genomics, Centro Cardiologico Monzino IRCCS, Milan, Italy
[d] Department of Biomedical, Surgical and Dental Sciences, University of Milan, Milan, Italy

ARTICLE INFO

*Keywords:*
Plaque vulnerability
Major adverse cardiac events (MACE)
Artificial intelligence
Coronary computed tomography angiography (CCTA)

ABSTRACT

Radiomics, the quantitative extraction and mining of features from radiological images, has recently emerged as a promising source of non-invasive image-based cardiovascular biomarkers, potentially revolutionizing diagnostics and risk assessment. This review explores its application within coronary plaques and pericoronary adipose tissue, particularly focusing on plaque characterization and cardiac events prediction. By shedding light on the current state-of-the-art, achievements, and prospective avenues, this review contributes to a deeper understanding of the evolving landscape of radiomics in the context of coronary arteries. Finally, open challenges and existing gaps are emphasized to underscore the need for future efforts aimed at ensuring the robustness and reliability of radiomics studies, facilitating their clinical translation.



## Introduction

Coronary artery disease (CAD) is a major cause of vascular morbidity and mortality worldwide, accounting for 8.9 million deaths annually [1]. The etiology is atherosclerosis, a chronic inflammatory-driven vascular disorder characterized by the formation of fatty plaques in the arterial wall [2]. Atherosclerotic plaques may become obstructive, determining impaired blood perfusion and resulting in stable angina pectoris. Alternatively, they may rupture or erode, leading to acute coronary syndrome, such as myocardial infarction (MI) [2]. The treatment can be pharmacological [3] or involve surgical or endovascular revascularization procedures [4]. Despite the high success rate of interventional procedures (90 % rate of 10-year survival free of cardiovascular mortality [5]), CAD is still a major cause of death and disability.

The challenge lies in the early identification of "vulnerable plaques", namely those prone to become culprit, such as rupture-prone, erosion-prone, hemorrhaging, or containing calcified nodules, as well as significantly stenotic plaques. These plaques are likely to cause major adverse cardiac events (MACE) or death, regardless their form, shape or stenosis [6–9]. A common subtype of rupture-prone plaque is the thin-cap fibroatheroma (TCFA), characterized by a large lipid-rich core surrounded by a thin fibrotic cap. When this cap undergoes transmural fissuring, it exposes the underlying thrombogenic and proinflammatory necrotic core to circulating blood [10]. Additionally, the presence of calcified nodules, compromising plaque integrity, is a typical characteristic of rupture-prone plaques [7]. Intravascular (e.g., intravascular ultrasound (IVUS), optical coherence tomography (OCT), near infrared spectroscopy) or non-invasive (e.g., coronary computed tomography angiography (CCTA)) imaging techniques enable the visualization of different high-risk plaque characteristics [11,12]. CCTA-based high-risk plaques identification relies on the presence of at least two of these adverse plaque characteristics: positive remodeling, low attenuation, spotty calcification, and 'napkin-ring' sign [13,14] (Fig. 1). Other CCTA-derived plaque characteristics (e.g., plaque presence, burden, composition, stenosis and location) have been used for the development of risk scores, as the coronary artery calcium, computed through the Agatston score [15], the segment stenosis score, grading coronary segments based on stenosis degree [16], and the segment involvement score, computed as the

* Corresponding author.
*E-mail address:* anna.corti@polimi.it (A. Corti).
[1] Authors contributed equally to the work and share first authorship.

https://doi.org/10.1016/j.tcm.2024.06.003

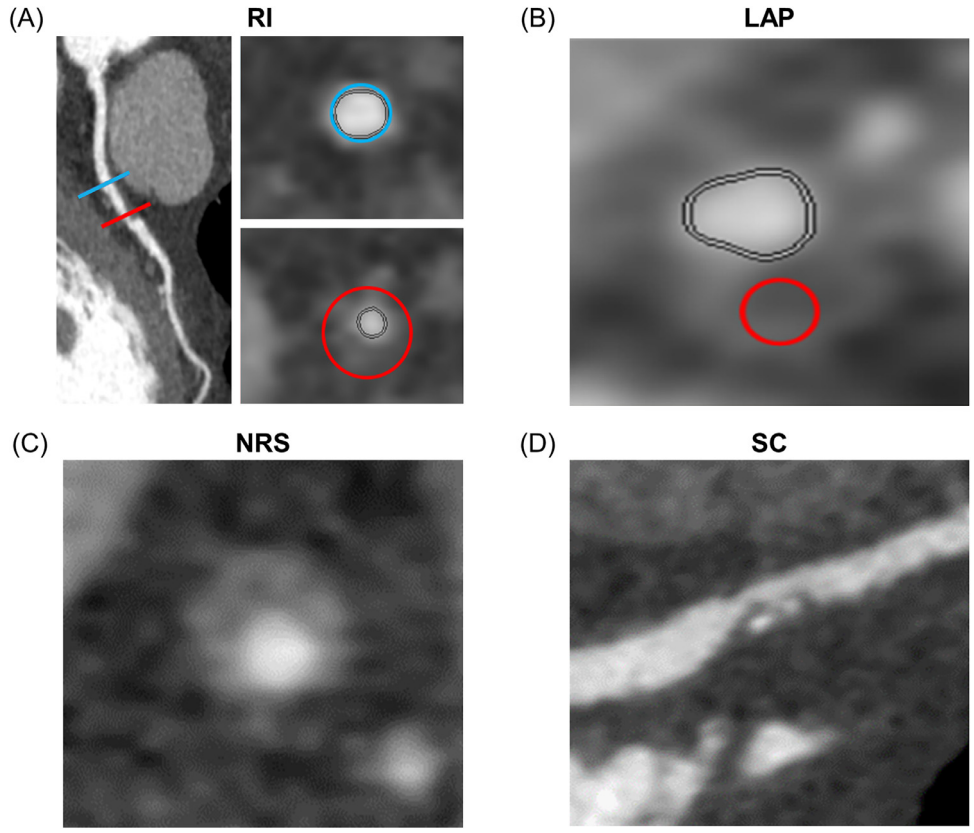


**Fig. 1.** High-risk plaque features: (A) plaque with positive remodeling index (RI), defined as RI > 1.1. RI is computed as the ratio between lesion plaque area (red circle) and reference lumen area (blue circle); (B) low attenuation plaque (LAP), associated with the presence of any voxel with < 30 Hounsfield Unit (HU); (C) mixed plaque with napkin-ring sign (NRS), characterized by the presence of rim-like thin enhancement (no more than 130 HU) distributed along the outer contour of the vessel and surrounding a fibro-lipidic plaque; (D) spotty calcification (SC), defined as any discrete calcification ≤ 3 mm in length and occupying ≤ 90° arc when viewed in short axis.

total number of coronary artery segments with plaque [16]. Other comprehensive risk-scores, with comparable capability in discriminating MACE [17], include the Coronary Artery Disease Reporting and Data System (CAD-RADS), based on stenosis severity and plaque burden [18], the CT-adapted Leaman score [19,20], based on composition, stenosis and location, or the Leiden CCTA score, based on presence, composition, stenosis and location [21].

Vascular inflammation has also emerged to be crucial in atherosclerotic plaque formation, progression, and rupture [22]. Systemic plasma biomarkers and proinflammatory cytokines have been largely adopted to assess vascular inflammation, but they are poorly associated with plaque vulnerability [23]. Recently, pericoronary adipose tissue (PCAT) has been identified as a sensor of coronary inflammation. Vascular inflammation inhibits lipid accumulation in PCAT preadipocytes, causing compositional changes in PCAT that can be detected by CCTA (Fig. 2) [24]. Accordingly, the fat attenuation index (FAI) has been proposed as imaging marker of vascular inflammation and plaque vulnerability [22].

Although the aforementioned image-derived characteristics are widely accepted as markers of plaque vulnerability, they alone are not sufficient to accurately stratify coronary plaques. It is now clear that plaque vulnerability is a complex, multifactorial condition, involving different biomechanical, structural/anatomical, and biological factors [8]. Accordingly, novel biomarkers of plaque vulnerability from different sources have been proposed, including biomechanical structural and fluid dynamic analyses, -omics data (e.g., genomics and proteomics), and imaging [25–27]. In this scenario, radiomics, namely the quantitative mining and extraction of features from clinical images, has recently emerged as a potential source of non-invasive image-based biomarkers for several cardio-

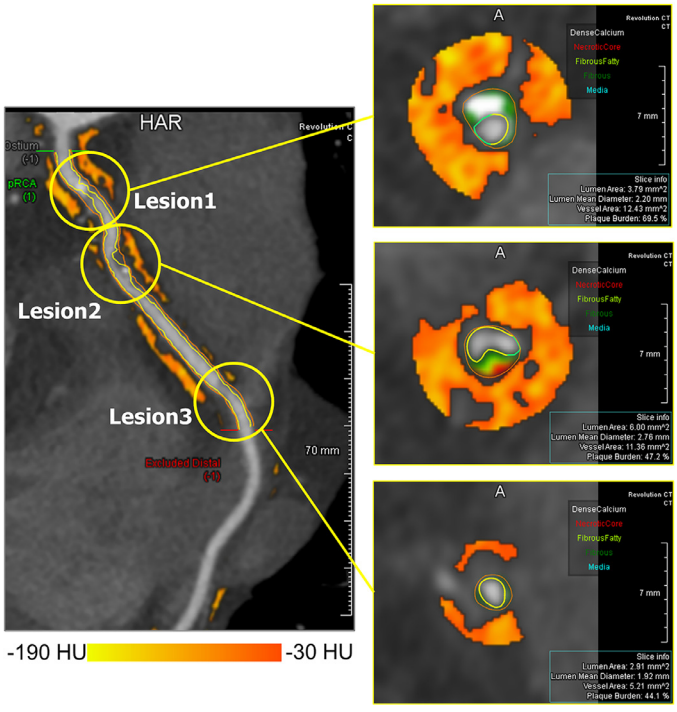


**Fig. 2.** Pericoronary adipose tissue attenuation in three lesions.

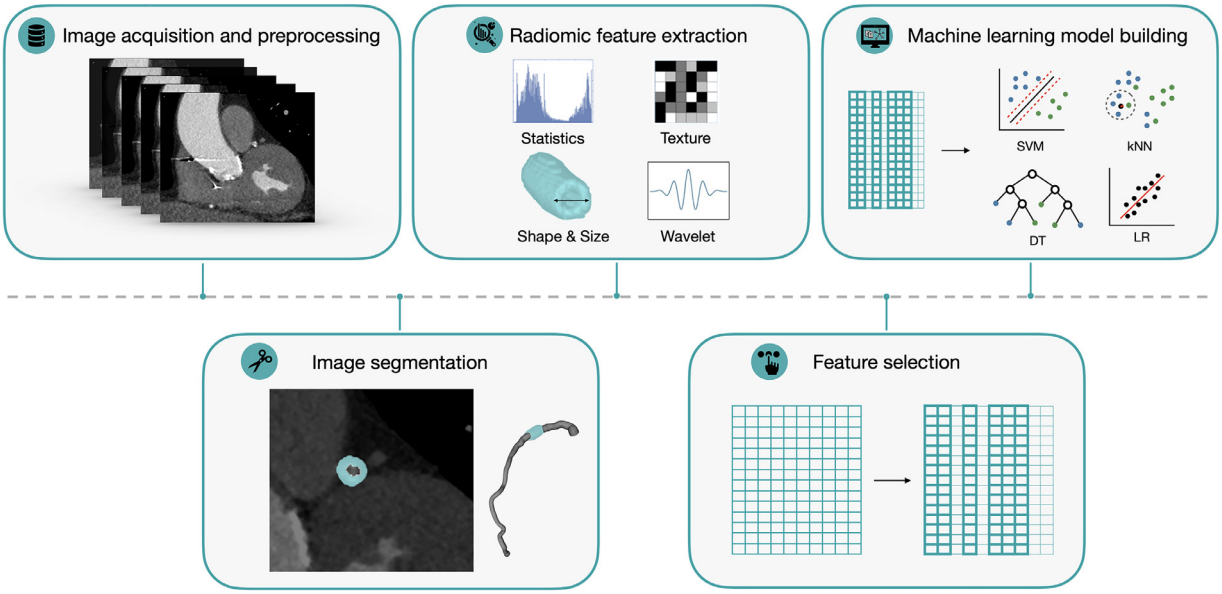


**Fig. 3.** Scheme of the radiomics workflow as applied to CCTA scans.

vascular applications [28]. Specifically, radiomics combined with machine learning (ML) methods has shown promise in identifying vulnerable coronary plaque biomarkers, predicting MACE, and developing fully-automatic plaque assessment tools supporting clinical diagnosis [29].

This paper provides an overview of the radiomic workflow, the current literature regarding the use of radiomics combined with ML approaches for plaque classification and MACE prediction (by considering applications on plaques and PCAT), and finally the open challenges for more robust and reliable radiomic analyses. The literature search was performed in PubMed, by considering keywords as “radiomics”, “coronary”, “plaque”.

## The radiomics approach

Radiomics is an emerging field for the identification of novel, non-invasive biomarkers from medical images. Radiomic features, extracted from a region of interest (ROI), provide quantitative information regarding ROI intensity, shape, and texture that are unrecognizable to the naked eye. Moreover, by capturing tissue characteristics and heterogeneity, radiomic features potentially embed relations with biological pathways and provide prognostic information enabling improved diagnosis, stratification, and clinical outcomes. The common radiomic workflow comprises: image acquisition and preprocessing, image segmentation, radiomic feature extraction and selection, and model training and validation (Fig. 3).

### *Image acquisition and preprocessing*

CCTA images can be acquired through CT scanners of different brands, type and generation, and various settings of the machine can be adopted, such as different voltages and amperages and the use of contrast agent. Moreover, different reconstruction parameters, such as slice thickness or filters, can be considered. To enable reproducibility of the radiomics approach, all this information should be provided transparently, as they may affect radiomic analysis [30–32]. In addition, to reduce image-related sources of variability, different image preprocessing steps are usually performed as z-score standardization or image resampling [33].

### *Image segmentation*

Image segmentation consists of the manual, semi-automatic or fully-automatic delineation of the ROI (or volume of interest, VOI). Since the ROI consists of the considered region for the extraction of the radiomic features, its accurate segmentation is essential for a reliable radiomic analysis. On one side, manual segmentation is time-consuming and, relying on radiologists’ expertise, inherently suffers from intra- and inter-reader variability, thus compromising the reproducibility of the radiomic analysis. On the other hand, fully automatic methods improve the objectivity and efficiency of the process, but their accuracy needs to be validated. Semi-automatic approaches emerge as a good balance between reproducibility and time commitment.

Manual segmentations of coronary plaques and PCAT are usually performed with open-source software such as 3D Slicer [34,35] or ITK-SNAP [36,37]. Semi-automated segmentation methodologies have also been reported, based on commercial software such as Autoplaque (Cedars-Sinai Medical Center, Los Angeles, CA, USA) for both coronary plaques and PCAT [38,39], Coronary Plaque Analysis (Syngo.Via, VB20, Siemens Healthineers) [29,40,41] and LIFEx [42] for coronary plaques, CoronaryDoc-FFR (Shukun Network Technology, Beijing) [43,44] for PCAT, or in-house software like TIMESlice [45].

A fully automatic deep learning approach has been proposed by Jin et al. [33], who applied a convolutional neural network (CNN) model to segment the coronary artery tree and detect plaque candidates. Compared with manual segmentation by radiologists, a Dice coefficient of 83 % was obtained, associated with the detection of all plaques (100 % sensitivity) along with a few false-positive candidates (78.9 % specificity and 70.3 % negative predictive value). Only one study used fully automatic segmentation of the coronary tree using commercial software (QAngioCT Research Edition; Medis Medical Imaging Systems B.V., Leiden, The Netherlands), but still the proximal and distal ends of each plaque were set manually [46].

### *Radiomic feature extraction*

Radiomic features, extracted from the ROI, are classified into 3 categories, namely shape and size, intensity, and textural fea-

tures. Shape and size features quantify the ROI spatial complexity, including information on the surface and volume and their relation (called compactness) up to fractal dimensions (enumerating self-symmetry). Intensity or first-order statistics features describe the frequency distribution of the pixel grey levels within the ROI (e.g., mean, minimum, standard deviation etc.). Textural features describe the spatial distribution of the grey levels, characterizing the texture and heterogeneity of the ROI. Such features are derived from textural matrices, considering different patterns of pixel grey level, such as the Gray Level Co-occurrence Matrix (describing, for each (i,j) element how many times a grey value j appears at a given distance from the grey value i), the Gray Level Run Length Matrix (quantifying grey level runs, which are defined as the length of consecutive pixels that have the same grey level value), the Gray Level Size Zone Matrix (quantifying grey level zones in an image, defined as a the number of connected voxels that share the same grey level intensity), the Neighboring Gray Tone Difference Matrix (quantifying the difference between a grey value and the average grey value of its neighbors within a distance) and the Gray Level Dependence Matrix (quantifying grey level dependencies in an image, defined as the number of connected voxels within a distance that are dependent on the center voxel). Intensity and textural features can be extracted either from the original images or from filtered versions of the images (obtained by applying filters such as Fourier or Wavelet transform), with about a hundred features extracted for each image version.

Nowadays, most radiomic analyses focus on three-dimensional features (e.g., features extracted from a volumetric ROI), in both coronary plaque [29,33,35,38,41,42,45] and PCAT studies [35,37,39,43,45,47,48]. However, examples of bi-dimensional coronary plaque radiomic analyses can be found [36,40], in which radiomic features were extracted from a bi-dimensional ROI. Different software can be used to extract radiomic features, including PyRadiomics (Python environment) [36,40,45,47], Radiomics Image Analysis (R environment) [38,39,42], Radiomics by Siemens Healthineers [29,40,41], CoronaryDoc [43], Artificial intelligence Kit by GE Healthcare [37], Research Portal V1.1 (United Imaging Intelligence, Co., Ltd.) [48], and TIMEslice [45].

*Feature selection*

To address the high dimensionality of data, feature selection approaches, based on filter or wrapper methods, are usually applied leading to the identification of a subset of stable, robust, and informative features. Filter methods are based on the feature relevance as measured by univariate statistics, hence independent on the classification model. Examples of studies that used only filter methods considered Spearman's correlation coefficient [40], intraclass correlation coefficient (ICC) [37], false positive rate test or familywise error rate test [38], minimum redundancy maximum relevance (MRMR) [41,45], and linear regression [39]. Wrapper methods iteratively select or eliminate features by training a model and evaluating its performance in cross-validation. Studies using wrapper methods alone include backward stepwise logistic regression (LR) [42] and least absolute shrinkage and selection operator (LASSO) LR [36,40,43]. The feature selection process may encompass several steps of the filter or wrapper methods, or both. Examples include the combination of the ICC analysis and the F-test [33], or the Boruta algorithm followed by XGBoost algorithm [29], LASSO regression and MRMR [48] (also with prior ICC evaluation [45]), ICC followed by univariate logistic analysis and Boruta algorithm [47], as well as the Analysis of Variance combined with the Recursive Feature Elimination and Relief method [35].

No single approach is inherently superior to others. Typically, various feature selection methods are assessed through internal validation, and the most effective one is subsequently applied to the test set. This process follows a partition of the training-test dataset, as detailed below.

*Machine learning model building*

Fig. 4 shows the optimal study design for ML models development. A training set should be used for feature selection process and model training, a validation set to identify optimal model parameters, and a test set to evaluate the performance of the model on unseen data. Performance on an independent external validation set should be assessed to further demonstrate the generalizability of the developed model. The optimal dataset partition (training, validation, and test set) has been used in a few studies [29,33,39,45]. Usually, due to the low sample size in the available datasets, the training-test partition is adopted and cross-validation is performed within the training test [35–38,40,43,47,48]. In some cases, cross-validation was performed on the entire dataset to fine-tune the model parameters [39,41]. However, this led to the generation of multiple ML models (with different parameters), whose performance on a new dataset was not tested, thus limiting their clinical applicability.

Usually, several models are trained and their performance in the validation set is compared to find the best one that will then be used in the test set. To quantify and compare the models, performance metrics are computed, based on the true positive (TP), false positive (FP), true negative (TN) and false negative (FN). The most used performance metrics are the sensitivity (i.e., true positive rate, or recall, computed as TP/(TP+FN)), specificity (i.e., true negative rate, computed as TN/(TN+FP)), accuracy (i.e., (TP+TN)/(TP+TN+FP+FN)), F1 score (i.e., 2TP/(2TP+FP+FN)), receiving operating curves (ROC, displaying the true positive rate vs. false positive rate (FPR)), and area under the curve (AUC).

Among the widely adopted models that perform well in the field of vulnerable plaque classification and MACE prediction are: regression models, such as LR [29,36,41,45,48], LR via LASSO [35], generalized LR [43], and least angle regression [38], and embedded models, such as random forest [40,45], eXtreme Gradient Boosting (XGBoost) [39,42], and gradient-boosting decision tree [33,37]. Moreover, linear support vector classifiers [35], decision trees [47], and Naïve Bayes [40] have demonstrated good performance. As for the feature selection methods, there is not a definitive superior algorithm among them. In standard practice, these algorithms undergo evaluation within an internal validation framework, and the most effective method is subsequently applied to the test set.

## Radiomics of coronary plaques

Below, state-of-the-art of radiomics studies on coronary plaques aimed at classifying plaques, identifying vulnerable plaques or predicting MACE, are reviewed, focusing on the objectives, study design, and key findings (Table 1). Moreover, a recently proposed scoring tool, METhodological RadiomICs Score (METRICS), was adopted to evaluate the methodological quality of the radiomic studies [30], with the score reported in Table 1.

*Plaque classification*

Two radiomic studies focused on the classification of plaques, depending on their composition [33,42]. Yunus et al. [42], developed a radiomic classifier for differentiating between calcified, non-calcified, mixed plaques and a control group, as labeled by expert radiologists. The dataset included 202 patients (with 163 normal arteries, 150 calcified, 85 non-calcified and 208 mixed plaques), divided into training and test sets. Four ML models were developed, considering (i) first-order, (ii) texture/second-order, (iii) shape, and (iv) all features as input. Model 1 (first-order features)

**Table 1**
Studies on radiomics of coronary plaque.

| Study | Aim | Dataset | Results | METRICS |
|---|---|---|---|---|
| Yunus et al., 2022 [42] | Plaque multiclass classification | Monocentric, mono-vendor<br>202 patients, 606 plaques<br>Random split training test (80 %–20 %) with 5-fold cross-validation on the training | a. First-order features model AUC = 0.91 (normal), AUC = 0.83 (calcified) AUC = 0.69 (non-calcified) AUC = 0.77 (mixed)<br>b. Textural features model AUC = 0.86 (normal) AUC = 0.78 (calcified) AUC = 0.72 (non-calcified) AUC = 0.74 (mixed)<br>c. Shape features model AUC = 0.50 (normal) AUC = 0.68 (calcified) AUC = 0.58 (non-calcified) AUC = 0.62 (mixed)<br>d. All radiomic features model AUC = 0.93 (normal) AUC = 0.82 (calcified) AUC = 0.69 (non-calcified) AUC = 0.76 (mixed) | 52.9 |
| Jin et al., 2022 [33] | 1. Calcific vs. non calcific plaque classification<br>2. Prediction of the stenosis grading | Multicentric, multi-vendor.<br>Training: 135 plaques<br>Validation: 50 plaques<br>Test: 52 plaques | 1. Plaque classification<br>Radiomic model AUC = 0.873<br>2. Plaque grading<br>Radiomic model AUC = 0.910 | 75.5 |
| Lin et al., 2022 [38] | Culprit vs. non-culprit plaque classification | Multicentric, mono-vendor<br>Training-validation-test: 180 plaques.<br>10-fold cross-validation<br>External Validation: 35 plaques | a. Radiomic + conventional plaque characteristics AUC = 0.86<br>b. conventional plaque model AUC = 0.76<br>*p = 0.004* | 69.9 |
| Chen et al., 2021 [41] | Identification of thin-cap fibroatheroma (TCFA) | Monocentric, mono-vendor<br>33 patients, 43 plaques. 5-fold cross-validation with 100 repeats | a. Radiomic model AUC = 0.952<br>b. Conventional plaque model AUC = 0.621<br>c. FAI AUC = 0.52<br>*p < 0.001 (a) vs. (b); (a) vs. (c); (b) vs. (c)* | 62.3 |
| Chen et al., 2023 [29] | 1. Identification of vulnerable plaques<br>2. MACE prediction. | Multicentric, multi-vendor<br>Vulnerability study<br>Training: 419 plaques<br>Test: 68 plaques<br>External validation: 47 plaques<br>MACE study<br>691 patients | 1. Plaque vulnerability<br>a. Radiomic model AUC = 0.80 (test)<br>b. Radiomic model AUC = 0.77 (external validation)<br>c. Radiomic + conventional plaque model AUC = 0.81 (entire dataset)<br>d. Conventional plaque model AUC = 0.73 (entire dataset)<br>*p < 0.01 (c) vs. (d)*<br>2. MACE prediction<br>e. Traditional cardiovascular risk C-index = 0.64<br>f. Traditional cardiovascular risk + CT parameters C-index = 0.69<br>g. Radiomic signature + traditional cardiovascular risk + CT parameters C-index = 0.72<br>*p < 0.01 (e) vs. (g); (f) vs. (g)* | 80.1 |
| Eslami et al., 2020 [34] | MACE prediction by 9 years | Multicentric, mono-vendor<br>Training: 318 patients. 3-fold cross-validation<br>Test: 306 patients | a. Radiomic signature AUC = 0.76<br>b. Radiomic signature + Agatston score AUC = 0.79<br>c. Agatston score AUC = 0.73<br>*p > 0.05*<br>A subset of patients with Agatston scores ≤ 300<br>d. Radiomic signature + Agatston score AUC = 0.80<br>e. Agatston score alone AUC = 0.63<br>*p = 0.03* | 71.2 |
| Hu et al., 2020 [36] | 1. Identification of hemodynamically significant plaques<br>2. MACE prediction by 1 year | Monocentric, multi-vendor<br>Training: 88 patients, 105 lesions.<br>Test: 31 patients | 1. Identification of hemodynamically significant plaque (training set)<br>a. Radiomic model AUC = 0.76<br>b. Conventional plaque model AUC = 0.63<br>*p = 0.058*<br>2. MACE prediction<br>c. Radiomic model AUC = 0.67<br>d. Conventional plaque model AUC = 0.59<br>*p = 0.441* | 59.5 |
| Li et al., 2021 [40] | Identification of hemodynamically significant plaques | Monocentric, mono-vendor<br>149 patients, 174 plaques.<br>Random split training test | a. Radiomic model AUC = 0.77<br>b. Conventional plaque model AUC = 0.77<br>*p = 0.58* | 62.1 |
| Kolossváry et al., 2019 [49] | Early vs. advanced atherosclerotic plaque classification | Monocentric, mono-vendor<br>7 hearts: 21 coronary arteries - 445 cross-sections<br>Random training-test split (75 %–25 %) with 5-fold cross-validation on the training set | a. Radiomic model AUC = 0.73<br>b. Visual assessment AUC = 0.65<br>c. Area of low attenuation AUC = 0.55<br>d. Average Hounsfield unit AUC = 0.53<br>*p<0.05 (a) vs. (b)* | 56.4 |
| Li et al., 2022 [50] | Vulnerable vs. non-vulnerable plaque classification | Monocentric, multi-vendor<br>Training: 36 hearts, 350 plaques, (with stratified 5-fold cross-validation)<br>Test: 8 hearts, 196 plaques | a. Radiomic models AUC = 0.78<br>b. Conventional plaque model AUC = 0.66<br>*p < 0.001* | 61.3 |

AUC: Area under the receiving operating characteristic curve; MI: myocardial infarction; CAD: coronary artery disease; TCFA: thin-cap fibroatheroma; MACE: major adverse cardiac event; FFR: fractional flow reserve; C-index: concordance index. METRICS: METhodological RadiomICs Score [30]

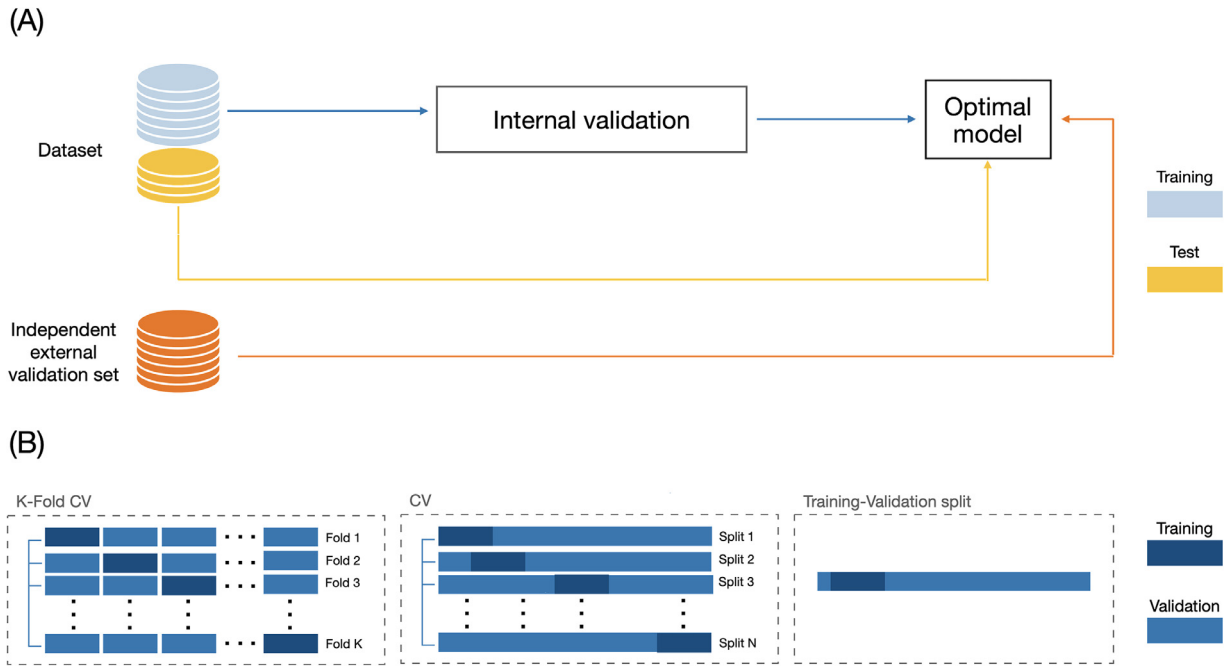


**Fig. 4.** Schematic representation of dataset partition for machine learning approaches. (A) The dataset is divided into a training set and test set; (B) internal validation can be performed via a k-fold cross-validation (CV), CV, or single split training-validation to obtain the optimal model.

performed best in classifying calcified (F1 score=0.78) and mixed plaques (F1 score=0.76) and, together with model 4, normal arteries (F1 score=0.88). Conversely, model 2 (texture/second order features) performed best in identifying non-calcified plaques (F1 score=0.63). The study provided insights into the role of radiomic feature classes in detecting plaque composition, with shape features emerging as irrelevant for plaque composition classification. Similarly, Jin et al. [33] proposed a radiomic approach to detect calcified vs. non-calcified and mixed plaques, and to predict the stenosis degree as labeled by radiologists. The study analyzed a multicenter, multivendor dataset of 237 plaques with different composition (149 calcified, 26 non-calcified, 62 mixed plaques) and degree of stenosis (31 with minimal, 122 with mild, 41 with moderate, 37 with severe stenosis and 6 occluded), partitioned into a training set (center 1), validation set (centers 2, 3, and 4), and test set (center 5). A deep learning approach was employed for image pre-processing (coronary artery segmentation, plaque candidate detection, and image patch extraction). Achieving an AUC~0.9, this approach enabled an automatic assessment of plaque composition and grading, significantly reducing the time required (56.2±5.7 s vs. 285.6±134.5 s, p=0.0001 for single-patient analysis by the automated tool and radiologist, respectively) while maintaining accuracy, reliability and generalizability.

*Plaque vulnerability and MACE prediction*

Within the context of plaque vulnerability, a study by Lin et al. [38] aimed to evaluate differences in radiomic features between culprit and non-culprit lesions in patients with MI or lesions in stable CAD patients. A dataset of 180 plaques in the training set and 35 plaques in the test set was considered (overall encompassing 79 culprit lesions in MI patients, 60 non-culprit lesions in MI patients, and 76 non-culprit lesions in stable CAD patients). Culprit lesions presented a unique radiomic phenotype compared with all non-culprit lesions or a subset of high-grade stenosis non-culprit lesions. The inclusion of the 18 most significant radiomic features in a ML model with conventional plaque characteristics (high-risk plaques by qualitative CCTA analysis, plaque volume, and volume and composition of low-density non-calcified plaques) provided better performance compared with conventional plaque analysis in discriminating culprit from non-culprit higher-grade stenosis plaques (AUC=0.86 vs. AUC=0.76; p=0.004). The relevance of these results is limited by the fact that culprit plaques were analyzed after MI. Consequently, (i) they might exhibit specific characteristics due to inflammation and (ii) the radiomic features identified to distinguish culprit plaques might be less effective for early prediction of vulnerable plaques before MI.

The identification of vulnerable plaques was also pursued by Chen et al. [29,41]. In a first study [41], the authors developed a radiomic model to identify TCFA as labeled through OCT, considering a dataset of 43 plaques (including 17 TCFA lesions). The model outperformed conventional plaque analysis and FAI in detecting TCFA, with an AUC of 0.95 vs. 0.62 and 0.52, respectively (p<0.001). Despite the smallness of the dataset and the use of 5-fold cross-validation (without a test set), the results highlighted the potential of CCTA radiomics in providing a non-invasive tool for better identification of vulnerable plaques than conventional CCTA-based plaque analysis. Later, the authors expanded the analysis by considering a multicentric dataset, with 419 plaques from center 1 (331 vulnerable, 88 non-vulnerable as defined by IVUS) for model development, 68 plaques from center 1 (64 vulnerable, 4 non-vulnerable) for model testing, and 47 plaques from centers 2-3 (32 vulnerable, 15 non-vulnerable), for external validation [29]. The developed radiomic signature provided an AUC=0.80 and AUC=0.77 on the internal and external test sets, respectively. Considering the entire dataset, adding the radiomic signature to conventional plaque features (high-risk plaques based on CCTA analysis, total plaque, non-calcified plaque, and necrotic core volume) improved the identification of vulnerable plaques compared to conventional plaque analysis alone (AUC=0.81 vs. AUC=0.73, p<0.01). Interestingly, in a prospective dataset of 691 patients (61 with MACE within a 3-year follow-up), the radiomic signature was independently associated with MACE (hazard ratio=2.01; p=0.005) and demonstrated enhanced prognostic performance (higher con-

cordance index) when combined with traditional cardiovascular risk factors and CT anatomical parameters, compared to cardiovascular risk factors alone or their combination with CT parameters ($p<0.01$). Despite these promising results, the radiomic signature had a high FPR, with only 12 % of patients with high radiomic signatures experiencing MACE, possibly due to a later stabilization of vulnerable plaques. To our knowledge, this study [29] represents the most relevant radiomic analysis of plaque vulnerability and MACE prediction to date, given the large dataset and the inclusion of both retrospective and prospective cohorts.

Regarding MACE prediction, two studies compared the effectiveness of radiomics to conventional plaque analysis but did not achieve promising results [34,36]. Eslami et al. [34] developed a radiomic signature of coronary artery calcium from cardiac CT in a cohort of 318 patients (30 MACE) and validated it in another cohort of 306 patients (29 MACE) with median follow-up time of 9.1 years, utilizing two cohorts of the Framingham Heart Study. Although the radiomic signature was significantly associated with MACE (hazard ratio=1.8, adjusted for Framingham risk score and Agatston score; p=0.01), it did not show superior discriminatory ability in predicting them compared to the Agatston score alone (AUC=0.76 vs. 0.73; p=0.25) or in combination with the Agatston score (AUC=0.79 vs. 0.73, p=0.05). Hu et al. [36] developed a radiomic model to identify significant ischemic plaques as defined by fractional flow reserve (FFR), using a dataset of 105 lesions (with 38 labelled as hemodynamically significant by FFR), and tested its predictive ability for MACE in 31 patients (15 with MACE). Although some trends were observed in the training dataset, the results were not significant in either identifying ischemic plaques or predicting MACE, as confirmed by a later study by Li et al. [40].

Ex-vivo *studies: plaque classification based on histological evaluation*

Two studies considered histological evaluation rather than other imaging modalities for plaque labelling, aiming to assess whether radiomics could serve as a non-invasive alternative for predicting histopathological outcomes [49,50]. Kolossvary et al. [49] showed that radiomics surpassed visual (based on plaque attenuation pattern) and quantitative (based on area of low attenuation and average Hounsfield units) assessments of *ex-vivo* CT cross-sections in identifying advanced atherosclerotic plaques as labeled by histological assessment. This prospective study involved 21 coronary arteries from 7 hearts, with the analysis of 445 cross-sections (30 % of which had advanced lesions). The dataset was partitioned into training and test sets and 8 different ML classifiers were trained and optimized using internal cross-validation on the training set. The best-performing model, applied to the test set, yielded an AUC=0.73, significantly higher than visual assessment, low attenuation area, and average HU ($p<0.05$). Despite its limitation of being based on only 7 hearts (with cross-sections from the same individuals, potentially biasing the results) and on CT images acquired from *ex-vivo* samples, the study indicated that radiomics is a promising, objective and non-invasive approach for better plaque stratification compared to current visual and histogram-based methods of assessment.

A similar *ex-vivo* analysis was performed by Li et al. [50], who developed a radiomics-based ML approach to identify vulnerable plaques labeled by histological evaluation. The study considered 350 plaque cross-sections from 36 transplanted hearts (200 of which with vulnerable plaques) for model training and development, and 196 plaque cross-sections from 8 transplanted hearts (132 of which with vulnerable plaques) for model testing. Two CCTA scanning equipment were used for the training and test sets. Eight classifiers were trained and the three best models were applied to the test set. All three models outperformed the conventional CCTA visual assessment in identifying vulnerable plaques, with an AUC$\in$[0.75-0.78] for the radiomic models and an AUC=0.66 for the conventional one ($p < 0.001$).

*Strengths and limitations*

An advanced frontier within CCTA radiomics of coronary plaques involves developing models to predict vulnerable plaques, as identified through invasive imaging techniques. Recent studies have yielded promising outcomes, underscoring the substantial superiority of radiomics over conventional plaque analysis in distinguishing vulnerable plaques. Among these studies, the investigation by Chen et al. [29] stands as the most sophisticated radiomic analysis. Notably, this study used a multi-centric and multivendor dataset and validated its findings on both test (AUC=0.80) and external validation (AUC=0.77) datasets. Nevertheless, further research using larger and prospective datasets is imperative to establish robust radiomic models capable of providing semi-automatic and reliable assessments of plaque vulnerability, potentially replacing traditional CCTA plaque analysis.

Concerning MACE prediction, the majority of proposed studies yielded results that were neither significant nor promising. An exception was observed in the study conducted by Chen et al. [29], where integrating radiomics with traditional risk factors and CT parameters notably enhanced prognostic performance. Given the limited number of studies addressing MACE prediction, additional investigations in this area are crucial for advancing the field.

As of now, in predicting hemodynamically significant plaques identified through invasive FFR, radiomic studies have not yielded significantly superior results when compared to conventional plaque analysis. This suggests the need for additional research endeavors to make advancements in this field.

In the context of plaque classification studies, while achieving commendable results (AUC>0.8), these models were developed by using the classification provided by expert radiologists as gold standard. Therefore, future efforts should prioritize the identification of plaque composition, as determined by invasive imaging modalities, to provide auxiliary tools for radiologists' activities.

Ultimately, *ex-vivo* radiomic studies derive their strength from using histological evaluation as the gold standard, aiming to establish radiomics as a non-invasive alternative for predicting pathological outcomes. Nevertheless, these analyses predominantly relied on cross-sections rather than complete plaque volumes and were limited by a restricted number of samples. Consequently, larger sample sizes and multicenter longitudinal studies will be needed to foster the development of more reliable and broadly applicable predictive radiomic models.

The assessment of the studies through the METRICS tool categorized 3 studies as "moderate" (with METRICS score between 40 % and 60 %), 6 as "good" (with METRICS score between 60 % and 80 %) and 1 nearly "excellent", with METRICS = 80.1 %. Most of the studies lacked multicentric analyses and external validation, provided insufficient reporting of image preprocessing methods, segmentation processes and features extraction details, did not perform features stability analysis and model calibration, and generally did not share codes or data.

## Radiomics of pericoronary adipose tissue

Below, state-of-the-art radiomic studies on PCAT, aimed at classifying plaque types, identifying hemodynamically significant plaques or predicting MACE, are reviewed, focusing on the aims, study design, and key findings (Table 2). Similarly to the plaque radiomic studies, the methodological quality of the PCAT radiomic analyses was assessed through METRICS [30], with the score reported in Table 2.

**Table 2**
Studies on radiomics of pericoronary adipose tissue.

| Study | Aim | Dataset | Results | METRICS |
|---|---|---|---|---|
| Jiang et al., 2022 [35] | 1. Normal vs. non-calcified plaque classification<br>2. Vulnerable vs. non-vulnerable non-calcified plaque classification | Monocentric, mono-vendor<br>431 patients<br>Random training-test split (70 %–30 %) | 1. normal vs. non-calcified<br>a. Radiomic model AUC = 0.83<br>b. Combined radiomic-clinical model AUC = 0.90<br>*p > 0.05*<br>2. vulnerable vs. non-vulnerable<br>c. Radiomic model AUC = 0.75<br>d. Combined radiomic-clinical model AUC = 0.75<br>*p > 0.05* | 57.3 |
| Wen et al., 2021 [47] | Identification of hemodynamically significant plaques | Monocentric, mono-vendor<br>121 plaques<br>Random training-test split (80 %–20 %). | a. Radiomic model AUC = 0.73<br>b. PCAT attenuation model AUC = 0.60<br>c. Combined radiomic + PCAT attenuation model AUC = 0.81<br>*p > 0.05 (a) vs. (b)*<br>*p = 0.015 (b) vs. (c)* | 56.2 |
| Zhou et al., 2023 [37] | Identification of hemodynamically significant plaques | Multicentric, mono-vendor<br>306 vessels<br>Random training-test split (75 %–25 %) | a. conventional model (plaque, EAT characteristics, and PCAT attenuation) AUC = 0.70<br>b. Radiomic model AUC = 0.74<br>c. Combined model (radiomic score + conventional features) AUC = 0.81<br>*p > 0.05 (a) vs. (b,c)*<br>*p = 0.012 (b) vs. (c)* | 66.3 |
| Yu et al., 2023 [44] | Identification of hemodynamically significant plaques | Monocentric, mono-vendor,<br>180 plaques<br>Random training-test split (66 %–34 %) | a. Radiomic model AUC = 0.74<br>b. CT-FFR model AUC = 0.79<br>c. Combined model AUC = 0.87<br>*p = 0.6 (a) vs. (b)*<br>*p < 0.05 (c) vs. (a) and (c) vs. (b)* | 55.6 |
| Oikonomou et al., 2019 [51] | MACE prediction by 5 years | Multicentric, multi-vendor<br>Training, validation, test: 202 patients. 80–20 % random stratified split<br>External validation: 1575 patients | a. Radiomic signature AUC = 0.77 (test)<br>b. Conventional model + radiomic signature AUC = 0.88 (external validation)<br>c. Conventional model AUC = 0.75 (external validation)<br>*p < 0.001 (b) vs. (c)* | 79.3 |
| Lin et al., 2020 [39] | Classification of patients with acute MI vs. stable CAD vs. no CAD | Monocentric, mono-vendor, 180 patients. 10-fold cross-validation | a. Clinical model: AUC = 0.76<br>b. Clinical + PCAT attenuation model AUC = 0.77<br>c. Clinical + PCAT attenuation + radiomic model AUC = 0.87<br>*p < 0.001 (a) vs. (c); (b) vs. (c)* | 65.9 |
| Si et al., 2022 [48] | Classification of patients with MI vs. UA | Monocentric, mono-vendor, 210 patients<br>Random training-test split (70 %–30 %)<br>5-fold cross-validation on training | a. LAD-radiomic model AUC = 0.8<br>b. LCx-radiomic model AUC = 0.88<br>c. RCA-radiomic model AUC = 0.88<br>d. FAI model AUC = 0.5<br>(*a,b,c*) vs. (d) p<0.0001<br>e. Combined radiomic-FAI model AUC = 0.95<br>*p < 0.05 (e) vs. (a,c,d); p > 0.05 (e) vs. (b)* | 65.3 |
| Wang et al., 2023 [45] | Classification of patients with MI vs. UA | Monocentric, multi-vendor, 216 patients. Training (116), validation (50) test (50) split based on date of admission | a. EAT radiomic model AUC = 0.69<br>b. RCA radiomic model AUC = 0.82<br>c. LAD radiomic model AUC = 0.76<br>d. LCx radiomic model AUC = 0.67<br>e. Combined radiomic model AUC = 0.86<br>*p < 0.05 (d) vs. (e)* | 56.8 |
| Dong et al., 2023 [43] | Classification of CAD vs. no CAD in patients with type 2 diabetes mellitus | Monocentric, mono-vendor, 229 patients.<br>Random training-test split (70 %–30 %) | a. Clinical model AUC = 0.69<br>b. Clinical + image model AUC = 0.93<br>c. Clinical + Radiomic model AUC = 0.69<br>d. Clinical + image + radiomic model AUC = 0.92<br>*p < 0.001 (a) vs. (b); (b) vs. (c); (d) vs. (a); (d) vs. (c)* | 49.8 |

PCAT: pericoronary adipose tissue; EAT: epicardial adipose tissue; AUC: Area under the receiving operating characteristic curve; MI: myocardial infarction; CAD: coronary artery disease; UA: unstable angina; MACE: major adverse cardiac event; FFR: fractional flow reserve; FAI: fat attenuation index; RCA: right coronary artery; LAD: left anterior descending artery; LCx: left circumflex artery. METRICS: METhodological RadiomICs Score [30]

*Plaque classification*

To our knowledge, only one study used PCAT-based radiomics to classify plaque types [35]. Jiang et al. [35] developed a PCAT-based radiomic model (proximal right coronary artery (RCA)) based on non-contrast CT scans to distinguish between normal arteries and non-calcified plaques, and further classify non-calcified plaques into vulnerable and non-vulnerable plaques (as labeled by CCTA). The study included 431 patients, among whom 173 had non-calcified plaques, including 59 with vulnerable plaques. The dataset was split into training (with internal cross-validation) and test cohorts. The radiomic model achieved an AUC=0.83 for distinguishing normal coronary arteries from non-calcified plaques, and an AUC=0.75 for differentiating vulnerable from non-vulnerable plaques. Incorporating clinical variables did not significantly improve performance. These findings suggested the feasibility of preliminary screening of patients with CAD using non-contrast CT scans, which are commonly used in clinical settings and do not require contrast agents, unlike CCTA.

*Identification of hemodynamically significant plaques*

PCAT-based radiomics has also been explored for identifying hemodynamically significant coronary artery stenosis, as assessed by invasive FFR [37,44,47]. In a study by Wen et al. [47], 121 lesions were evaluated, with 55 identified as hemodynamically sig-

nificant. CCTA-based radiomic models were developed considering PCAT features extracted from left anterior descending artery (LAD), RCA, and left circumflex artery (LCx) and compared with a model based on visual evaluation of PCAT attenuation. Additionally, a combined model incorporating the best radiomic model with PCAT attenuation was developed. Although the radiomic models did not significantly outperform the PCAT attenuation model alone, their combination resulted in significantly higher performance than the PCAT attenuation model alone (AUC=0.81 vs. 0.60, p=0.015). Despite being derived from a relatively small and single-center dataset, these results demonstrated the added value of PCAT radiomics in non-invasively identifying hemodynamically significant lesions, potentially reducing the need for unnecessary FFR measurements. Similar results were obtained by Zhou et al. [37], who developed a PCAT-based radiomic model to diagnose hemodynamically significant lesions (labeled by FFR) and compared its performance with a conventional model based on plaque features, EAT characteristics, and PCAT attenuation, using a multicentric dataset of 306 vessels (124 of which were labeled as hemodynamically significant) divided into training-test sets. The AUCs of the radiomic and conventional models were not significantly different, but combining the radiomic score with conventional features significantly enhanced diagnostic performance compared to the conventional model (AUC=0.81 and 0.70, p=0.012). A recent study by Yu et al. involving 180 lesions (68 of which were hemodynamically significant) [44], further evaluated the diagnostic performance of PCAT-based radiomics versus CT-FFR and the combination of both in detecting hemodynamically significant lesions. CT-FFR predictions were derived from a ML model trained on computational fluid-dynamic simulations previously conducted in coronary arteries reconstructed from CCTA. Interestingly, PCAT-based radiomics demonstrated comparable performance to CT-FFR, positioning it as a feasible alternative to the more computationally demanding CT-FFR approach. Moreover, their combination resulted in a significantly higher AUC compared to the single models (combined model AUC=0.87 vs. radiomic model AUC=0.74 and CT-FFR model AUC=0.79, p<0.05).

Overall, these findings confirmed the potential of PCAT-based radiomics in improving the detection of hemodynamically significant lesions.

*MACE prediction*

One of the earliest and most comprehensive investigations of PCAT radiomics was conducted by Oikonomou et al. [51], focusing on the prognostic capability of a PCAT-based radiomic signature in predicting MACE by 5 years. The PCAT-based radiomic signature was developed using a multicentric dataset, composed of 202 patients (101 with MACE) for model training, validation and internal testing (80–20 % split) and further validated on a prospective external validation set of 1575 patients (432 with MACE or late revascularization), from the CRISP-CT and SCOT-HEART trials [52,53]. In the internal test set, the radiomic signature achieved an AUC=0.77 for predicting MACE and significantly stratified high-risk from low-risk patients when an optimal threshold was applied (HR=10.84). Moreover, when integrated into a conventional model based on clinical factors, the AUC significantly improved compared to the conventional model alone on the external validation set (AUC=0.88 vs. AUC=0.75, p<0.001). Finally, the developed PCAT radiomic signature showed significant differentiation in 44 patients with acute MI compared to 44 matched controls (p<0.001), further validating the predictive power of PCAT radiomics.

Lin et al. [39] further investigated the capability of CCTA-based PCAT radiomics to differentiate patients with acute MI from those with stable or absent CAD. The study included 60 patients with MI, 60 with stable CAD, and 60 without CAD. PCAT was segmented around the proximal RCA and, for MI patients, also around culprit and non-culprit lesions. A preliminary statistical analysis revealed that patients with acute MI exhibited a distinct PCAT radiomic phenotype, with 182 features significantly differing from patients with stable CAD and 224 features distinct from individuals without CAD, out of 1103 analyzed radiomic variables. These differences predominantly involved textural and shape features. Using a cross-validation on the entire dataset, the authors developed three ML models, based on (i) clinical features, (ii) clinical features and PCAT attenuation, and (iii) clinical features, PCAT attenuation, and radiomic features. The third model outperformed both the second and first models (AUC=0.87, AUC=0.77, and AUC=0.76, respectively, p<0.001). Interestingly, the authors also found that radiomic features did not significantly differ between culprit and non-culprit lesions in patients with MI, suggesting that patients with MI have diffuse coronary inflammation globally affecting PCAT regardless lesion location. Furthermore, PCAT radiomic features in MI patients did not present significant changes at a 6-month follow-up, suggesting that coronary inflammation resulted in irreversible PCAT modifications. Overall, these results demonstrate the potential of PCAT radiomics in understanding coronary inflammation and characterizing MI patients.

A similar study was performed by Si et al. [48] to evaluate the ability of PCAT-based radiomics in distinguishing patients with MI from those with unstable angina (n=105 patients for both groups). PCAT was segmented from the RCA, LAD, and LCx, and FAI was computed. Five models were developed: a FAI model comprising FAI values of the three coronary arteries, three separate radiomic models (one for each coronary artery), and a combined model, integrating the scores from FAI model and the radiomic model. A random training-test split of the dataset was applied. PCAT radiomics demonstrated superiority in identifying MI patients compared to the FAI model (LAD-radiomic AUC=0.85, LCx-radiomic AUC=0.88, RCA-radiomic AUC=0.88, FAI model AUC=0.50; p<0.0001). The combined model achieved an AUC=0.95, although not significantly different from the LCx-radiomic model. These results further support the potential of PCAT radiomics in characterizing patients with MI.

Differently, Wang et al. [45] focused exclusively on patients with non-ST-segment elevation MI (NSTEMI), who are more difficult to diagnose than patients with ST-segment elevation MI and have symptoms similar to patients with unstable angina, but with myocardial cell necrosis. A dataset of 108 NSTEMI patients and 108 patients with unstable angina was considered and divided into training, validation, and test cohorts. Five models were developed, based on radiomic features extracted from epicardial adipose tissue (EAT) or from PCAT of the RCA, LAD, and LCx as well as the combination of these three PCAT radiomic models. While in the validation cohort, the combined model significantly outperformed the EAT, LAD, and LCx models, in the test cohort a significant difference was found only compared to the LCx model (AUC=0.86, AUC=0.69, AUC=0.82, AUC=0.76, and AUC=0.67 for the combined, EAT, RCA, LAD, and LCx models). Overall, the results were consistent with the previous studies [39,48] and suggested that PCAT-based radiomics has potentials in stratifying patients with NSTEMI or unstable angina.

Despite the promising results presented so far, PCAT radiomics has shown limited performance in identifying CAD in patients with type 2 diabetes mellitus, as evidenced by a recent study by Dong et al. [43]. The authors found that a model based only on clinical factors and CT image parameters had superior performance (AUC=0.93) compared to the model based on clinical factors and PCAT radiomic features (AUC=0.69), p<0.001. Moreover, the combined model integrating clinical factors, CT image parameters, and radiomic features, achieved a high performance (AUC=0.92) but did not significantly outperform the model based on clinical fac-

tors and CT image parameters alone (p=0.776), indicating that the addition of radiomic features did not improve discrimination ability. The authors attributed this finding to the peculiar aspects characterizing patients with type 2 diabetes mellitus, as the high coronary inflammation, potentially affecting PCAT.

*Strengths and limitations*

In the context of identifying hemodynamically significant plaques assessed via invasive FFR, PCAT radiomics demonstrated comparable performance to conventional PCAT analysis, and their combination exhibited superiority. Notably, only one study utilized PCAT radiomics for plaque classification, producing results consistent with other studies on plaque radiomics. Regarding MACE prediction, several studies reported AUC>0.8 in discriminating MI, notably superior to clinical or FAI-based models. However, most studies were based on monocentric and relatively small datasets. An exception was observed in the study by Oikonomou et al. [51], which yielded significant results, demonstrating the potentiality of PCAT-radiomics in predicting MACE, considering a multicentric dataset from the CRISP-CT and SCOT-HEART trials.

The assessment of the studies through the METRICS tool revealed 5 studies rated as “moderate” (with METRICS score between 40 % and 60 %) and 4 studies rated as “good” (with METRICS score between 60 % and 80 %). Compared to the plaque radiomics, PCAT radiomics studies presented more limitations, such as frequent absence of internal testing and usage of standardized features extraction software. Overall, PCAT radiomics is currently less advanced compared to plaque radiomics, with fewer studies and more preliminary investigations. This could be attributed to several factors: first, in CAD investigations, the plaque typically represents the primary focus of analysis (being directly implicated in the pathology), and this is mirrored in radiomic studies; second, PCAT has only recently started to receive greater attention from the research community; third, identifying and segmenting PCAT is more challenging. Future efforts should be focused on addressing these challenges and utilizing larger and prospective datasets to develop robust, generalizable, and validated PCAT-based radiomic models.

## Challenges and future directions

With the advancement in imaging techniques, coupled with progress in AI methods and increased computational power, radiomics has emerged as a powerful AI-driven quantitative image analysis technique for high-throughput data mining and extraction from medical images. Radiomics has recently found applications in cardiovascular medicine, showing its potential as a source of non-invasive markers of plaque and PCAT heterogeneity and texture. These markers enable the identification of predictors of vulnerable coronary plaque and MACE. This review underscores that comprehensive radiomic analysis of plaque and PCAT improves the identification of vulnerable plaques and generally outperform traditional plaque analyses in stratifying patients into high and low-risk categories, with only a few exceptions.

Hence, radiomics holds the potential to establish a non-invasive, automated, and objective methodology for accurately assessing high-risk coronary plaques, marking a significant advancement in precision cardiovascular medicine. However, translating radiomics into clinical practice faces challenges due to the current lack of standardized and generalized approaches. The radiomic pipelines are indeed susceptible to various sources of variabilities, including differences in image acquisition protocols, segmentation issues (intra and inter-observer variability for manual segmentation), image preprocessing steps, and methods used for feature extraction. These challenges, coupled with inadequate and non-transparent reporting methodologies, impede the reproducibility, generalizability, and validation of radiomic analyses. To address these limitations and work towards establishing a consensus on radiomic methodologies, several initiatives have been launched. For instance, the “Image Biomarker Standardization Initiative” [54] focuses on features standardization, while initiatives as the Radiomics Quality Score [55] or METRICS [30] aims to assess the quality of radiomic studies. Additionally, TRIPOD (transparent reporting of a multivariable prediction model for individual prognosis or diagnosis) [56] provides best practice guidelines for reporting prognostic models. While many of these guidelines and initiatives originated in the context of oncological radiomics, and although some aspects are generally applicable, specific protocols need to be developed to address the unique challenges posed by coronary plaque studies. Herein we conducted an evaluation of radiomic studies through the METRICS tool [30]. Our findings indicate that most of the studies are based on single-center datasets, lack a transparent description of the image preprocessing steps and segmentation methods, omit radiomic features stability analysis, often do not perform external validation and rarely provide access to codes or data. Overall, although several guidelines have been proposed to standardize radiomic studies, adherence to these guidelines appears to be generally low, demonstrating the ongoing need for additional efforts in this regard. Moreover, there is a pressing need to establish specific standardized reporting guidelines tailored for radiomic studies focusing on vulnerable coronary plaques, to improve the consistency and reproducibility of research findings.

In addition to concerns about the reproducibility of radiomic pipelines, another challenge relates to data availability and quality, which are pivotal for the development of robust radiomic models. Most of the radiomic studies reviewed herein relied on relatively small, unbalanced, and monocentric datasets. Collaborative initiatives and the use of large-scale, multicentric datasets can overcome the challenge of limited data availability, thereby enhancing the development and validation of radiomic models.

Despite the aforementioned limitations, this research field is undeniably expanding and making a noteworthy contribution to the identification of vulnerable coronary plaques. Given that plaque vulnerability is a complex, multifactorial condition, influenced by the concurrent action of different biological and biomechanical factors [8], integrating data from different sources at multiple levels is expected to offer a more comprehensive assessment of plaque characteristics. This integrated approach could potentially enhance the accuracy and effectiveness of plaque stratification. From a biomechanical perspective, both structural mechanics and hemodynamic factors have been proposed as predictors of plaque progression and vulnerability. Combining these factors with image-derived morphological factors has been found to increase predictive performance [25]. Additionally, circulating biomarkers, such as high sensitivity C-reactive protein, creatinine, tumor necrosis factor-$\alpha$, and interleukin-6, have demonstrated efficacy in stratifying high-risk plaques, defined by intravascular imaging [57]. Furthermore, a recent study has identified 72 genes associated with coronary plaque rupture through gene correlation network analysis [26]. However, to date, a comprehensive, multilevel approach that integrates biomechanics, radiomics, circulating biomarkers, and genetic data for accurate stratification of high-risk coronary plaques remains elusive. Such an approach (Fig. 5) could represent a breakthrough in predicting plaque vulnerability, overcoming the limitations of current strategies, that typically consider vulnerability markers separately. This integrated approach could facilitate personalized management of CAD in both its early and advanced stages. Indeed, developing and validating novel combined individual cardiovascular risk "signatures" could enable better and earlier identification of patients at high risk of MACE. Implementing such integration into a user-friendly interface, where CCTA images serve as input and yield a highly accurate multiparametric definition of

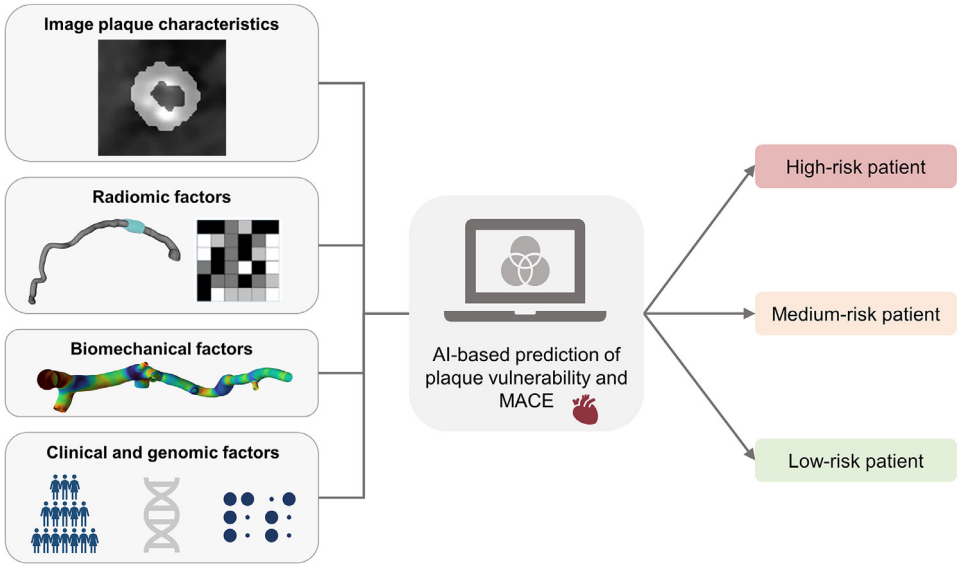


**Fig. 5.** Future multilevel approach integrating image plaque characteristics, radiomics, biomechanics, clinical and genomic data for accurate stratification of vulnerable patients.

the vessel lesion as output, could reduce end-user hands-on time and enhance image visualization and interpretation for early diagnosis.

## Conclusions

Radiomics-based ML methods for the identification of high-risk coronary plaques are still in the early developmental stages. However, the current state-of-the-art indicates a growing interest in leveraging radiomic markers for plaque vulnerability, supported by promising results. Overall, plaque and PCAT radiomics have demonstrated superior capability in detecting vulnerable plaques and effectively stratifying high/low-risk patients compared to conventional plaque analysis.

Radiomics promises to pave the way for a non-invasive, automated, and objective approach for accurate assessment of high-risk coronary plaques, providing a major contribution to the field of precision cardiovascular medicine. However, future studies based on large, multicenter datasets are imperative to further validate the radiomic approach. In addition, substantial efforts should be directed at standardizing and generalizing the radiomics pipeline.

Finally, integrating clinical, biological, radiomic, and biomechanical information is considered essential to define an accurate and individualized risk stratification criterion. This holistic approach has the potential to enhance patient care by enabling early identification and targeted management of individuals at risk for MACE.

## Data availability statement

No new data were generated or analyzed in support of this research

## Ethical statement

We the undersigned declare that this manuscript is original, has not been published before and is not currently being considered for publication elsewhere.

We confirm that the manuscript has been read and approved by all named authors and that there are no other persons who satisfied the criteria for authorship but are not listed. We further confirm that the order of authors listed in the manuscript has been approved by all of us.

We confirm that all authors are responsible for the content and have read and approved the manuscript; and that the manuscript conforms to the Uniform Requirements for Manuscripts Submitted to Biomedical Journals published in Annals in Internal Medicine

We understand that the Corresponding Author is the sole contact for the Editorial process. He/she is responsible for communicating with the other authors about progress, submissions of revisions and final approval of proofs.

## Declaration of competing interest

Gianluca Pontone declares the following conflict of interest: Honorarium as speaker/consultant and/or research grant from GE Healthcare, Bracco, Heartflow, Boheringher. All other authors do not report any conflicts.

## CRediT authorship contribution statement

**Anna Corti:** Writing – review & editing, Writing – original draft, Methodology, Investigation, Formal analysis, Conceptualization. **Francesca Lo Iacono:** Writing – review & editing, Writing – original draft, Methodology, Investigation. **Francesca Ronchetti:** Writing – review & editing, Methodology. **Saima Mushtaq:** Writing – review & editing. **Gianluca Pontone:** Writing – review & editing, Investigation. **Gualtiero I. Colombo:** Writing – review & editing, Investigation. **Valentina D.A. Corino:** Writing – review & editing, Supervision, Investigation, Conceptualization.

## Funding

This work has been supported by Fondazione Regionale per la Ricerca Biomedica (Regione Lombardia), project 3432721 - AI-CORPS. AC is funded by the National Plan for NRRP Complementary Investments (PNC, established with the decree-law 6 May 2021, n. 59, converted by law n. 101 of 2021) in the call for the funding of research initiatives for technologies and innovative trajectories in the health and care sectors (Directorial Decree n. 931 of 06-06-2022) - project n. PNC0000003 - AdvaNced Technologies for Human-centrEd Medicine (project acronym: ANTHEM). This work reflects only the authors' views and opinions, neither the Ministry for University and Research nor the European Commission can be considered responsible for them.

## References


[1] Global, regional, and national age-sex-specific mortality for 282 causes of death in 195 countries and territories, 1980-2017: a systematic analysis for the Global Burden of Disease Study 2017. Lancet 2018;392:1736–88 (London, England). doi:10.1016/S0140-6736(18)32203-7.

[2] Bentzon JF, Otsuka F, Virmani R, Falk E. Mechanisms of plaque formation and rupture. Circ Res 2014;114:1852–66. doi:10.1161/CIRCRESAHA.114.302721.

[3] van Veelen A, van der Sangen NMR, Henriques JPS, Claessen B. Identification and treatment of the vulnerable coronary plaque. Rev Cardiovasc Med 2022;23:39. doi:10.31083/j.rcm2301039.

[4] Lawton JS, Tamis-Holland JE, Bangalore S, Bates ER, Beckie TM, Bischoff JM, et al. 2021 ACC/AHA/SCAI guideline for coronary artery revascularization: a report of the American college of cardiology/American heart association joint committee on clinical practice guidelines. J Am Coll Cardiol 2022;79:e21–129. doi:10.1016/j.jacc.2021.09.006.

[5] Vieira RD, Hueb W, Gersh BJ, Lima EG, Pereira AC, Rezende PC, et al. Effect of complete revascularization on 10-year survival of patients with stable multivessel coronary artery disease: MASS II trial. Circulation 2012;126:S158–63. doi:10.1161/CIRCULATIONAHA.111.084236.

[6] Naghavi M, Libby P, Falk E, Casscells SW, Litovsky S, Rumberger J, et al. From vulnerable plaque to vulnerable patient: a call for new definitions and risk assessment strategies: part I. Circulation 2003;108:1664–72. doi:10.1161/01.CIR.0000087480.94275.97.

[7] Stefanadis C, Antoniou C, Tsiachris D, Pietri P. Coronary atherosclerotic vulnerable plaque: current perspectives. J Am Heart Assoc 2017;6:1–18. doi:10.1161/JAHA.117.005543.

[8] Lee KY, Chang K. Understanding vulnerable plaques: current status and future directions. Korean Circ J 2019;49:1115–22. doi:10.4070/kcj.2019.0211.

[9] Gaba P, Gersh BJ, Muller J, Narula J, Stone GW. Evolving concepts of the vulnerable atherosclerotic plaque and the vulnerable patient: implications for patient care and future research. Nat Rev Cardiol 2023;20:181–96. doi:10.1038/s41569-022-00769-8.

[10] Kolodgie FD, Burke AP, Farb A, Gold HK, Yuan J, Narula J, et al. The thin-cap fibroatheroma: a type of vulnerable plaque: the major precursor lesion to acute coronary syndromes. Curr Opin Cardiol 2001;16:285–92. doi:10.1097/00001573-200109000-00006.

[11] Stefanadis C, Antoniou CK, Tsiachris D, Pietri P. Coronary atherosclerotic vulnerable plaque: current perspectives. J Am Heart Assoc 2017;6. doi:10.1161/JAHA.117.005543.

[12] Bom MJ, van der Heijden DJ, Kedhi E, van der Heyden J, Meuwissen M, Knaapen P, et al. Early detection and treatment of the vulnerable coronary plaque: can we prevent acute coronary syndromes? Circ Cardiovasc Imaging 2017;10. doi:10.1161/CIRCIMAGING.116.005973.

[13] Kolossváry M, Szilveszter B, Merkely B, Maurovich-Horvat P. Plaque imaging with CT-a comprehensive review on coronary CT angiography based risk assessment. Cardiovasc Diagn Ther 2017;7:489–506. doi:10.21037/cdt.2016.11.06.

[14] Opincariu D, Benedek T, Chițu M, Raț N, Benedek I. From CT to artificial intelligence for complex assessment of plaque-associated risk. Int J Cardiovasc Imaging 2020;36:2403–27. doi:10.1007/s10554-020-01926-1.

[15] Agatston AS, Janowitz WR, Hildner FJ, Zusmer NR, Viamonte MJ, Detrano R. Quantification of coronary artery calcium using ultrafast computed tomography. J Am Coll Cardiol 1990;15:827–32. doi:10.1016/0735-1097(90)90282-t.

[16] Min JK, Shaw LJ, Devereux RB, Okin PM, Weinsaft JW, Russo DJ, et al. Prognostic value of multidetector coronary computed tomographic angiography for prediction of all-cause mortality. J Am Coll Cardiol 2007;50:1161–70. doi:10.1016/j.jacc.2007.03.067.

[17] van den Hoogen IJ, van Rosendael AR, Lin FY, Lu Y, Dimitriu-Leen AC, Smit JM, et al. Coronary atherosclerosis scoring with semiquantitative CCTA risk scores for prediction of major adverse cardiac events: propensity score-based analysis of diabetic and non-diabetic patients. J Cardiovasc Comput Tomogr 2020;14:251–7. doi:10.1016/j.jcct.2019.11.015.

[18] Cury RC, Leipsic J, Abbara S, Achenbach S, Berman D, Bittencourt M, et al. CAD-RADS™ 2.0 - 2022 coronary artery disease-reporting and data system: an expert consensus document of the society of cardiovascular computed tomography (SCCT), the American college of cardiology (ACC), the American college of radiology (ACR), and the N. J Cardiovasc Comput Tomogr 2022;16:536–57. doi:10.1016/j.jcct.2022.07.002.

[19] Mushtaq S, De Araujo Gonçalves P, Garcia-Garcia HM, Pontone G, Bartorelli AL, Bertella E, et al. Long-term prognostic effect of coronary atherosclerotic burden: validation of the computed tomography-Leaman score. Circ Cardiovasc Imaging 2015;8:e002332. doi:10.1161/CIRCIMAGING.114.002332.

[20] Andreini D, Pontone G, Mushtaq S, Gransar H, Conte E, Bartorelli AL, et al. Long-term prognostic impact of CT-Leaman score in patients with non-obstructive CAD: Results from the COronary CT Angiography EvaluatioN For Clinical Outcomes InteRnational Multicenter (CONFIRM) study. Int J Cardiol 2017;231:18–25. doi:10.1016/j.ijcard.2016.12.137.

[21] van Rosendael AR, Shaw LJ, Xie JX, Dimitriu-Leen AC, Smit JM, Scholte AJ, et al. Superior risk stratification with coronary computed tomography angiography using a comprehensive atherosclerotic risk score. JACC Cardiovasc Imaging 2019;12:1987–97. doi:10.1016/j.jcmg.2018.10.024.

[22] Antonopoulos AS, Sanna F, Sabharwal N, Thomas S, Oikonomou EK, Herdman L, et al. Detecting human coronary inflammation by imaging perivascular fat. Sci Transl Med 2017;9. doi:10.1126/scitranslmed.aal2658.

[23] Margaritis M, Antonopoulos AS, Digby J, Lee R, Reilly S, Coutinho P, et al. Interactions between vascular wall and perivascular adipose tissue reveal novel roles for adiponectin in the regulation of endothelial nitric oxide synthase function in human vessels. Circulation 2013;127:2209–21. doi:10.1161/CIRCULATIONAHA.112.001133.

[24] Oikonomou EK, Antoniades C. The role of adipose tissue in cardiovascular health and disease. Nat Rev Cardiol 2019;16:83–99. doi:10.1038/s41569-018-0097-6.

[25] Lv R, Wang L, Maehara A, Guo X, Zheng J, Samady H, et al. Image-based biomechanical modeling for coronary atherosclerotic plaque progression and vulnerability prediction. Int J Cardiol 2022;352:1–8. doi:10.1016/j.ijcard.2022.02.005.

[26] Xu BF, Liu R, Huang CX, He BS, Li GY, Sun HS, et al. Identification of key genes in ruptured atherosclerotic plaques by weighted gene correlation network analysis. Sci Rep 2020;10:10847. doi:10.1038/s41598-020-67114-2.

[27] Lin A, Manral N, McElhinney P, Killekar A, Matsumoto H, Kwiecinski J, et al. Deep learning-enabled coronary CT angiography for plaque and stenosis quantification and cardiac risk prediction: an international multicentre study. Lancet Digit Heal 2022;4:e256–65. doi:10.1016/S2589-7500(22)00022-X.

[28] Kolossváry M, De Cecco CN, Feuchtner G, Maurovich-Horvat P. Advanced atherosclerosis imaging by CT: Radiomics, machine learning and deep learning. J Cardiovasc Comput Tomogr 2019;13:274–80. doi:10.1016/j.jcct.2019.04.007.

[29] Chen Q, Pan T, Wang YN, Schoepf UJ, Bidwell SL, Qiao H, et al. A coronary CT angiography radiomics model to identify vulnerable plaque and predict cardiovascular events. Radiology 2023;307:e221693. doi:10.1148/radiol.221693.

[30] Kocak B, Akinci D, Antonoli T, Mercaldo N, Alberich-Bayarri A, Baessler B, Ambrosini I, et al. METhodological RadiomICs Score (METRICS): a quality scoring tool for radiomics research endorsed by EuSoMII. Insights Imaging 2024;15:8. doi:10.1186/s13244-023-01572-w.

[31] Kolossváry M, Szilveszter B, Karády J, Drobni ZD, Merkely B. Maurovich-Horvat P. Effect of image reconstruction algorithms on volumetric and radiomic parameters of coronary plaques. J Cardiovasc Comput Tomogr 2019;13:325–30. doi:10.1016/j.jcct.2018.11.004.

[32] Berenguer R, Pastor-Juan MDR, Canales-Vázquez J, Castro-García M, Villas MV, Mansilla Legorburo F, et al. Radiomics of CT features may be nonreproducible and redundant: influence of CT acquisition parameters. Radiology 2018;288:407–15. doi:10.1148/radiol.2018172361.

[33] Jin X, Li Y, Yan F, Liu Y, Zhang X, Li T, et al. Automatic coronary plaque detection, classification, and stenosis grading using deep learning and radiomics on computed tomography angiography images: a multi-center multi-vendor study. Eur Radiol 2022;32:5276–86. doi:10.1007/s00330-022-08664-z.

[34] Eslami P, Parmar C, Foldyna B, Scholtz JE, Ivanov A, Zeleznik R, et al. Radiomics of coronary artery calcium in the framingham heart study. Radiol Cardiothorac Imaging 2020;2:e190119. doi:10.1148/ryct.2020190119.

[35] Jiang XY, Shao ZQ, Chai YT, Liu YN, Li Y. Non-contrast CT-based radiomic signature of pericoronary adipose tissue for screening non-calcified plaque. Phys Med Biol 2022;67. doi:10.1088/1361-6560/ac69a7.

[36] Hu W, Wu X, Dong D, Cui LB, Jiang M, Zhang J, et al. Novel radiomics features from CCTA images for the functional evaluation of significant ischaemic lesions based on the coronary fractional flow reserve score. Int J Cardiovasc Imaging 2020;36:2039–50. doi:10.1007/s10554-020-01896-4.

[37] Zhou K, Shang J, Guo Y, Ma S, Lv B, Zhao N, et al. Incremental diagnostic value of radiomics signature of pericoronary adipose tissue for detecting functional myocardial ischemia: a multicenter study. Eur Radiol 2023;33:3007–19. doi:10.1007/s00330-022-09377-z.

[38] Lin A, Kolossváry M, Cadet S, McElhinney P, Goeller M, Han D, et al. Radiomics-based precision phenotyping identifies unstable coronary plaques from computed tomography angiography. JACC Cardiovasc Imaging 2022;15:859–71. doi:10.1016/j.jcmg.2021.11.016.

[39] Lin A, Kolossváry M, Yuvaraj J, Cadet S, McElhinney PA, Jiang C, et al. Myocardial infarction associates with a distinct pericoronary adipose tissue radiomic phenotype: a prospective case-control study. JACC Cardiovasc Imaging 2020;13:2371–83. doi:10.1016/j.jcmg.2020.06.033.

[40] Li L, Hu X, Tao X, Shi X, Zhou W, Hu H, et al. Radiomic features of plaques derived from coronary CT angiography to identify hemodynamically significant coronary stenosis, using invasive FFR as the reference standard. Eur J Radiol 2021;140:109769. doi:10.1016/j.ejrad.2021.109769.

[41] Chen Q, Pan T, Yin X, Xu H, Gao X, Tao X, et al. CT texture analysis of vulnerable plaques on optical coherence tomography. Eur J Radiol 2021;136:109551. doi:10.1016/j.ejrad.2021.109551.

[42] Yunus MM, Mohamed Yusof AK, Ab Rahman MZ, Koh XJ, Sabarudin A, Nohuddin PNE, et al. Automated classification of atherosclerotic radiomics features in coronary computed tomography angiography (CCTA). Diagnostics 2022;12 (Basel, Switzerland). doi:10.3390/diagnostics12071660.

[43] Dong X, Li N, Zhu C, Wang Y, Shi K, Pan H, et al. Diagnosis of coronary artery disease in patients with type 2 diabetes mellitus based on computed tomography and pericoronary adipose tissue radiomics: a retrospective cross-sectional study. Cardiovasc Diabetol 2023;22:14. doi:10.1186/s12933-023-01748-0.

[44] Yu L, Chen X, Ling R, Yu Y, Yang W, Sun J, et al. Radiomics features of pericoronary adipose tissue improve CT-FFR performance in predicting hemodynamically significant coronary artery stenosis. Eur Radiol 2023;33:2004–14. doi:10.1007/s00330-022-09175-7.

[45] Wang Z, Zhang J, Zhang A, Sun Y, Su M, You H, et al. The role of epicardial and pericoronary adipose tissue radiomics in identifying patients with non-ST-segment elevation myocardial infarction from unstable angina. Heliyon 2023;9:e15738. doi:10.1016/j.heliyon.2023.e15738.

[46] Kolossváry M, Park J, Bang JI, Zhang J, Lee JM, Paeng JC, et al. Identification of invasive and radionuclide imaging markers of coronary plaque vulnerability using radiomic analysis of coronary computed tomography angiog-

raphy. Eur Hear J Cardiovasc Imaging 2019;20:1250–8. doi:10.1093/ehjci/jez033.
[47] Wen D, Xu Z, An R, Ren J, Jia Y, Li J, et al. Predicting haemodynamic significance of coronary stenosis with radiomics-based pericoronary adipose tissue characteristics. Clin Radiol 2022;77:e154–61. doi:10.1016/j.crad.2021.10.019.
[48] Si N, Shi K, Li N, Dong X, Zhu C, Guo Y, et al. Identification of patients with acute myocardial infarction based on coronary CT angiography: the value of pericoronary adipose tissue radiomics. Eur Radiol 2022;32:6868–77. doi:10.1007/s00330-022-08812-5.
[49] Kolossváry M, Karády J, Kikuchi Y, Ivanov A, Schlett CL, Lu MT, et al. Radiomics versus visual and histogram-based assessment to identify atheromatous lesions at coronary CT angiography: an *ex vivo* study. Radiology 2019;293:89–96. doi:10.1148/radiol.2019190407.
[50] Li XN, Yin WH, Sun Y, Kang H, Luo J, Chen K, et al. Identification of pathology-confirmed vulnerable atherosclerotic lesions by coronary computed tomography angiography using radiomics analysis. Eur Radiol 2022;32:4003–13. doi:10.1007/s00330-021-08518-0.
[51] Oikonomou EK, Williams MC, Kotanidis CP, Desai MY, Marwan M, Antonopoulos AS, et al. A novel machine learning-derived radiotranscriptomic signature of perivascular fat improves cardiac risk prediction using coronary CT angiography. Eur Heart J 2019;40:3529–43. doi:10.1093/eurheartj/ehz592.
[52] Oikonomou EK, Marwan M, Desai MY, Mancio J, Alashi A, Hutt Centeno E, et al. Non-invasive detection of coronary inflammation using computed tomography and prediction of residual cardiovascular risk (the CRISP CT study): a post-hoc analysis of prospective outcome data. Lancet 2018;392:929–39 (London, England). doi:10.1016/S0140-6736(18)31114-0.
[53] Newby DE, Adamson PD, Berry C, Boon NA, Dweck MR, Flather M, et al. Coronary CT angiography and 5-year risk of myocardial infarction. N Engl J Med 2018;379:924–33. doi:10.1056/NEJMoa1805971.
[54] Zwanenburg A, Vallières M, Abdalah MA, Aerts H, Andrearczyk V, Apte A, et al. The image biomarker standardization initiative: standardized quantitative radiomics for high-throughput image-based phenotyping. Radiology 2020;295:328–38. doi:10.1148/radiol.2020191145.
[55] Lambin P, Leijenaar RTH, Deist TM, Peerlings J, de Jong EEC, van Timmeren J, et al. Radiomics: the bridge between medical imaging and personalized medicine. Nat Rev Clin Oncol 2017;14:749–62. doi:10.1038/nrclinonc.2017.141.
[56] Collins GS, Reitsma JB, Altman DG, Moons KGM. Transparent reporting of a multivariable prediction model for individual prognosis or diagnosis (TRIPOD): the TRIPOD statement. BMJ 2015;350:g7594. doi:10.1136/bmj.g7594.
[57] Nakajima A, Libby P, Mitomo S, Yuki H, Araki M, Seegers LM, et al. Biomarkers associated with coronary high-risk plaques. J Thromb Thrombolysis 2022;54:647–59. doi:10.1007/s11239-022-02709-2.